On the Group Delay Effect of DSN Microwave Components on Multimegabit Telemetry

P. J. Lee
Communications Systems Research Section

*In this article a method of determining the group delay effect of DSN microwave components on multimegabit telemetry detection is described. That is, when the gain and phase shift characteristics of the overall system between the modulator and demodulator are given, the group delay effect for the intended data rate can be assessed by examining the equation for the recovered signal (equation *) for several rectangular pulse inputs with different duty cycles. For example, the group delay loss of 30 Mbit/sec telemetry with only a Block II X-band maser is less than 0.2 dB even with a 10-MHz center frequency offset.*

I. Introduction

A simplified model for the transmission and reception of multimegabit telemetry is shown in Fig. 1. The modulating signal $x(t)$ is a unit amplitude random binary data signal with bit duration T_b. The phase-modulated signal $y(t)$ is

$$y(t) = K \sin [2\pi f_c t + \phi x(t)]$$

where $f_c (=1/T_c)$ is the carrier frequency ($T_c << T_b$), and ϕ is the modulation index. The K in $y(t)$ is the signal amplitude, and will be taken as unity for convenience. If the channel is ideal, then $r(t) = y(t)$,

$$y(t) \cos (2\pi f_c t - \beta_1) = \sin (\phi x(t) + \beta_1) + \sin (4\pi f_c t + \phi x(t) - \beta_1)$$

and

$$\hat{x}(t) = \sin (\phi x(t) + \beta_1)$$

where β_1 is the phase difference between the two reference oscillators at the modulator and demodulator and will also be ignored for later calculations. The modulation index ϕ is *usually* chosen to be less than $\pi/2$ for both maximizing energy of recovered signal $\hat{x}(t)$ and efficient carrier referencing. Since we are only interested in the modulation component, we assume $\phi = \pi/2$.

The overall system between the modulator and demodulator (any combinations of amplifiers, mixers, diplexers, filters, antennas, waveguides, transmission lines, etc.) can be considered as an effective channel bandpass filter. Typical gain and phase shift characteristics of the resulting channel are shown in Fig. 2. Let f_0 be the center of frequency of BPF; $g(f)$ and $\beta(f)$ are the relative gain and phase shift at frequency f to those at f_0. Usually they have symmetry such that

$$g(f_0 - \Delta f) = g(f_0 + \Delta f) \text{ and } \beta(f_0 - \Delta f) = -\beta(f_0 + \Delta f) .$$

It is well known that when a signal $y(t)$ containing components throughout the frequency band of the BPF is divided into a set of narrowband signals, each of these will be subject to a different time delay. Hence the output signal must have a different waveform from the input, and phase distortion appears along with the amplitude distortion.

It is very difficult to analyze the effect of group delay for a random data signal. Hence for analysis we suggest the use of periodic rectangular pulse modulating signals with period $Ts(=1/fs = nT_b)$ and duty cycle $1/n$, for several different n's, instead of the actual random data signal. Since in most cases the bit time-bandwidth product BT_b is not smaller than one, the group delay together with amplitude distortion of one bit affects only itself and its adjacent neighbors.

In the next section, we describe the way of finding the recovered signal $\hat{x}(t)$ including the case where the center frequency of the effective bandpass filter is not matched to the carrier frequency of the incoming signal. Then we show that the group delay effect can be determined by the losses of the integrated values of $\hat{x}(t)$ with group delay compared to those of $\hat{x}(t)$ without group delay.

II. The Recovered Signal $\hat{x}(t)$

The Fourier series representation of a periodic signal $z(t)$ with period $T(=1/f)$ is

$$z(t) = \sum_{k=-\infty}^{\infty} Z(kf)\, e^{jk2\pi ft} \underset{\mathscr{F}^{-1}}{\overset{\mathscr{F}}{\rightleftharpoons}} Z(kf) = \frac{1}{T} \int_T z(t)\, e^{-jk2\pi ft}\, dt .$$

Let $f_c = mnf_s$ $(T_s = mnT_c)$ where m represents the number of carrier cycles per bit time and n represents the number of bit times over which the bit stream is periodic. The m and n are assumed to be integers so that $y(t)$ is also a periodic signal with period T_s (see Fig. 3) and the Fourier series representation can be used. Then $y(t)$ with $f_c = mnf_s$ and its kth Fourier coefficient $Y_{mn}(kf_s)$ are

$$y(t) = \sin\left[2\pi mnf_s t + \frac{\pi}{2}\, x(t)\right]$$

where

$$x(t) = \begin{cases} 1, 0 \leqslant |t - \ell Ts| < T_s/2n \\ -1, T_s/2n \leqslant |t - \ell T_s| < T_s/2 \end{cases} \qquad \ell = 0, \pm 1, \pm 2, \ldots,$$

and

$$Y_{mn}(kf_s) = \frac{\sin[(mn-k)\pi/n]}{(mn-k)\pi} + \frac{\sin[(mn+k)\pi/n]}{(mn+k)\pi} - \frac{\sin[(mn-k)\pi]}{(mn-k)2\pi} - \frac{\sin[(mn+k)\pi]}{(mn+k)2\pi}$$

Note that

$$Y_{mn}(-kf_s) = Y_{mn}(kf_s) \text{ and } Y_{mn}(mnf_s) \approx \frac{1}{\pi}\left(\frac{1}{n} - \frac{1}{2}\right).$$

Also, when $mn >> \ell > 0$

$$Y_{mn}[(mn+\ell)f_s] \approx Y_{mn}[(mn-\ell)f_s] \approx \frac{\sin(\ell\pi/n)}{\ell\pi}$$

Therefore

$$y(t) \approx \left(\frac{1}{n} - \frac{1}{2}\right)\cos(mn2\pi f_s t) + \sum_{\ell=1}^{m'} \frac{\sin(\ell\pi/n)}{\ell} \{\cos[(mn+\ell)2\pi f_s t] + \cos[(mn-\ell)2\pi f_s t]\}$$

where m' is some number less than $mn/2$. Also

$$r(t) \approx \left(\frac{1}{n} - \frac{1}{2}\right)\cos(mn2\pi f_s t)$$

$$+ \sum_{\ell=1}^{m''} \frac{\sin(\ell\pi/n)}{\ell} \cdot \Big(g[(mn+\ell)f_s] \cdot \cos\{(mn+\ell)2\pi f_s t - \beta[(mn+\ell)f_s]\}$$

$$+ g[(mn-\ell)f_s] \cdot \cos\{(mn-\ell)2\pi f_s t - \beta[(mn-\ell)f_s]\}\Big)$$

where m'' is determined by the bandwidth of BPF which is usually much less than m'.

Then finally

$$\hat{x}(t) = \text{const.} + \sum_{\ell=1}^{m''} \frac{\sin(\ell\pi/n)}{\ell} \Big(g[(mn+\ell)f_s] \cos\{\ell 2\pi f_s t - \beta[(mn+\ell)f_s]\}$$

$$+ g[(mn-\ell)f_s] \cos\{\ell 2\pi f_s t + \beta[(mn-\ell)f_s]\}\Big)$$

$$= \text{const.} + \sum_{\ell=1}^{m''} \frac{\sin(\ell\pi/n)}{\ell} R_{mn}^{(\ell)} \cos\left(\ell 2\pi f_s t - \theta_{mn}^{(\ell)}\right) \qquad (*)$$

where

$$R_{mn}^{(\ell)} = \Big(g^2[(mn+\ell)f_s] + g^2[(mn-\ell)f_s] + 2g[(mn-\ell)f_s] \cdot g[(mn-\ell)f_s]$$

$$\cdot \cos\{\beta[(mn+\ell)f_s] + \beta[(mn-\ell)f_s]\}\Big)^{1/2}$$

and

$$\theta_{mn}^{(\ell)} = \tan^{-1}\left(\frac{g[(mn+\ell)f_s]\ \sin\ \{\beta[(mn+\ell)f_s]\} - g[(mn-\ell)f_s]\ \sin\ \{\beta[(mn-\ell)f_s]\}}{g[(mn+\ell)f_s]\ \cos\ \{\beta[(mn+\ell)f_s]\} + g[(mn-\ell)f_s]\ \cos\ \{\beta[(mn-\ell)f_s]\}}\right).$$

The additive constant is just the dc bias term. If the BPF has symmetry, i.e., $g(f_0 - \Delta f) = g(f_0 + \Delta f)$ and $\beta(f_0 - \Delta f) = -\beta(f_0 + \Delta f)$ and if $f_0 = f_c$, then $R_{mn}^{(\ell)} = 2g((mn + \ell)f_s)$ and $\theta_{mn}^{(\ell)} = \beta[(mn + \ell)f_s]$.

III. Example and Conclusion

To see the group delay effect on 30 Mbit/sec telemetry with a Block II X-band maser, the shapes of $\hat{x}(t)$ are shown in Figs. 4 and 5 for n = 2 and 10 respectively, using the data from Fig. 6 of Ref. 1 and equation (*) with $f_c = f_0$ (m = 281). The same signal conditions are repeated in Figs. 6 and 7 with $f_c = f_0$ −15 MHz. The dotted lines in Fig. 4 to Fig. 7 are the shapes of $\hat{x}(t)$'s without group delay; i.e., only amplitude distortions are considered. When we use an integrator for detection of $\hat{x}(t)$ with integrating duration T_s/n, the losses of the integrated values of $\hat{x}(t)$ with group delay compared to those of $\hat{x}(t)$ without group delay are shown in Fig. 8 for various center frequency offsets. From these observations, we can conclude that the group delay effect on 30 Mbit/sec telemetry with Block II X-band maser is not significantly deleterious even with a substantial center frequency offset.

Reference

1. Trowbridge, D. L., "X-band Traveling Wave Maser Amplifier," in *DSN Progress Report 42-28*, Jet Propulsion Laboratory, Pasadena, Calif., pp. 69-77.

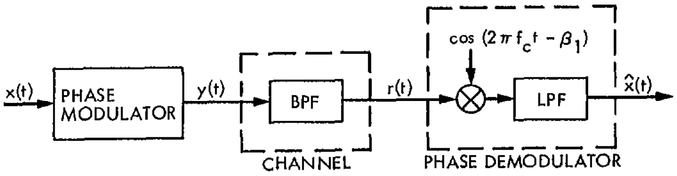

Fig. 1. System model

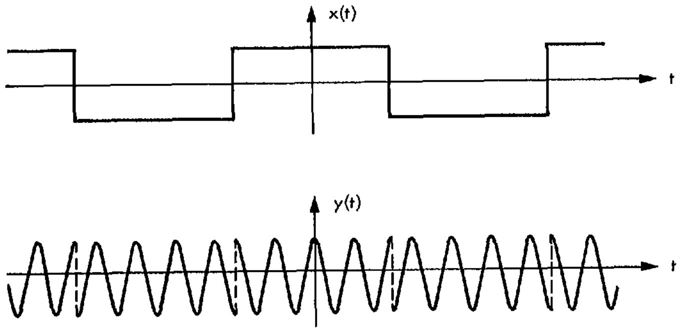

Fig. 3. Example of modulating and modulated signal, n = 2, m = 4

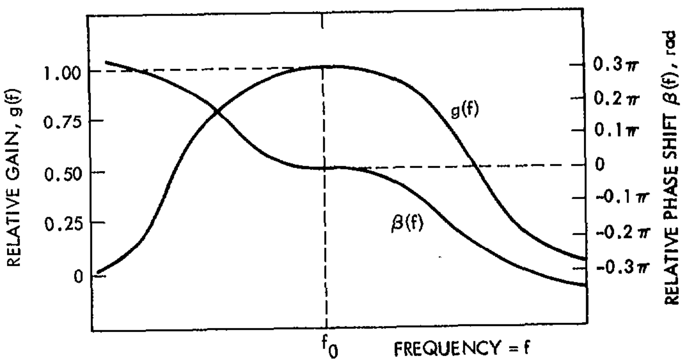

Fig. 2. Typical gain and phase shift characteristics of the channel

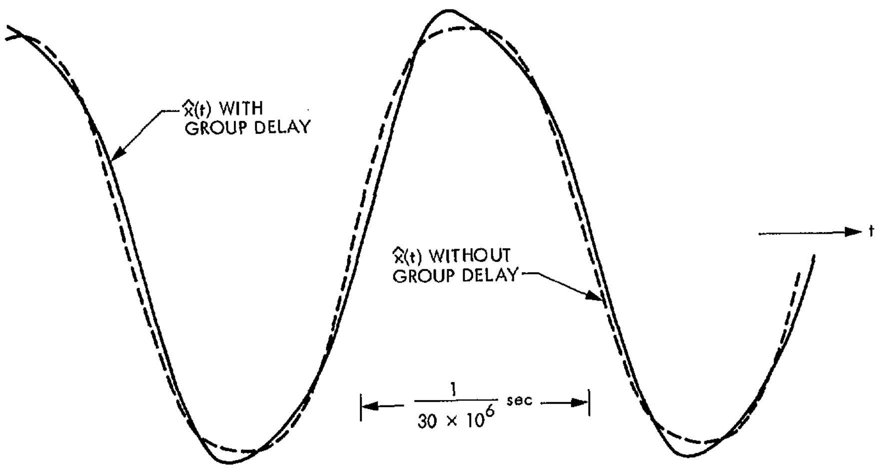

Fig. 4. The shapes of $\hat{x}(t)$, n = 2, f_c = f_0

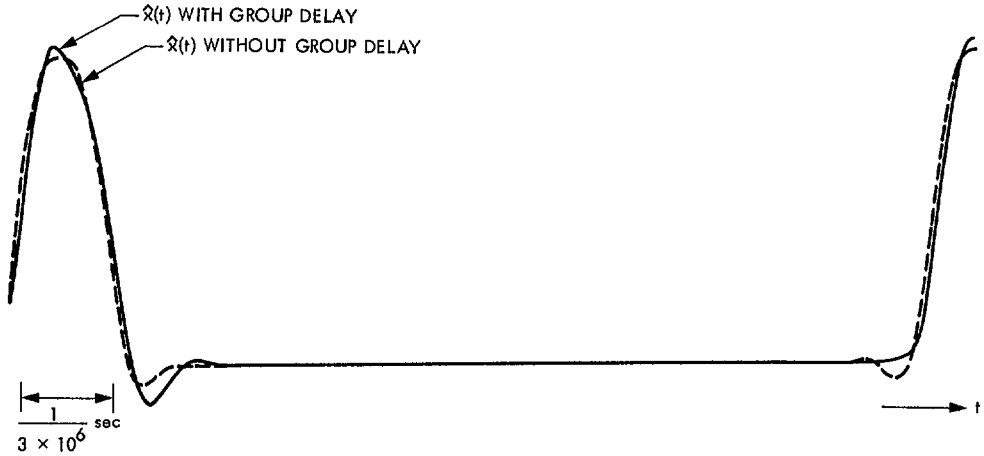

Fig. 5. The shapes of $\hat{x}(t)$, $n = 10$, $f_c = f_0$

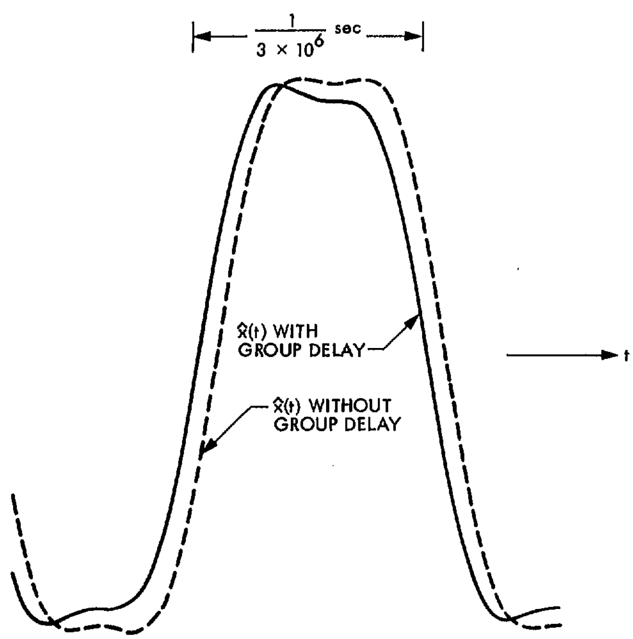

Fig. 6. The shapes of $\hat{x}(t)$, $n = 2$, $f_c = f_0 - 15$ MHz

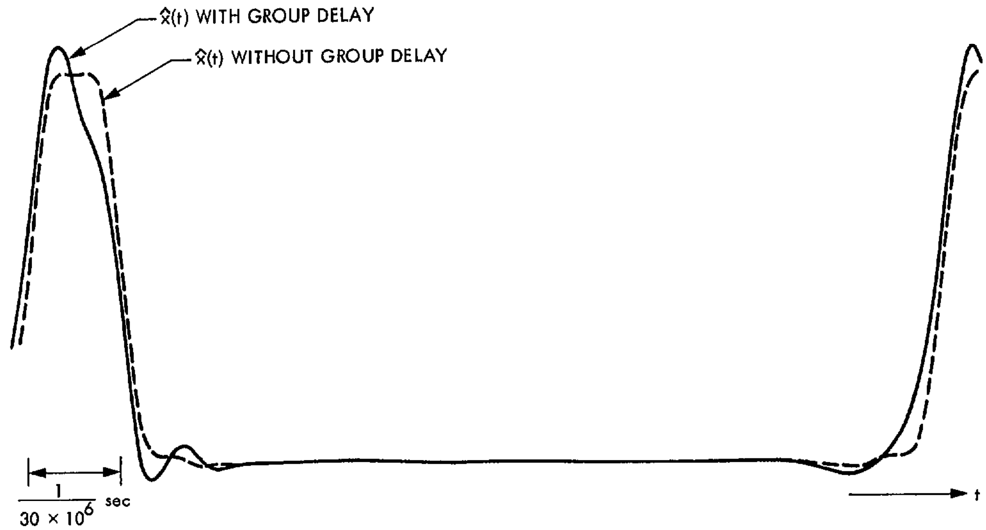

Fig. 7. The shapes of $\hat{x}(t)$, n = 10, $f_c = f_0 - 15$ MHz

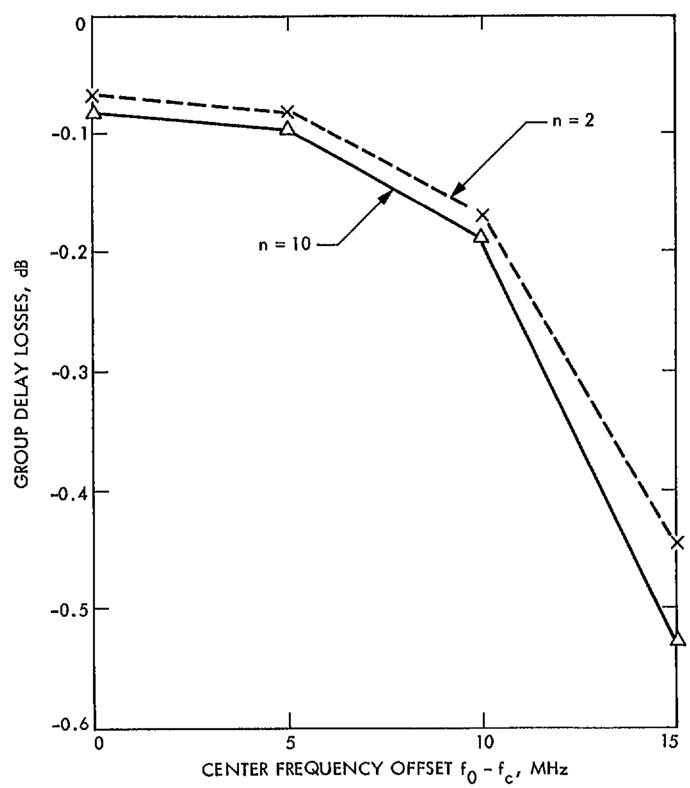

Fig. 8. Group delay losses vs center frequency offset